Theorical analysis of a monolithic all-active three-section semiconductor laser

Mohammed Mehdi Bouchene,[*1] Rachid Hamdi,[1] and Qin Zou[2]

[1] *Laboratoire des Télécommunications (LT), Faculté des Sciences et de la Technologie, Université 8 mai 1945 Guelma, 24000-Bp.401, Algeria*
[2] *Institut Mines-Télécom, Télécom SudParis, UMR 5157 CNRS, Université Paris-Saclay, 9 rue Charles Fourier, 91011 Evry Cedex, France*

Abstract—We propose a novel semiconductor laser structure. It is composed of three cascaded active sections: a Fabry-Pérot laser section sandwiched between two gain-coupled distributed feedback (DFB) laser sections. We have modeled this multi-section structure. The simulation results show that compared with index- and gain-coupled DFB lasers, a significant reduction in elongitudinal spatial-hole burning can be obtained with the proposed device, and this is what leads to a stable single longitudinal mode operation at relatively high optical power with a SMSR exceeding 56dB.

Multi-section semiconductor lasers have attracted considerable attention because of their unique properties such as a wide wavelength tuning range [1], high-speed direct modulation [2], and resulting applications. In recent years, various structures of multi-section laser diodes have been proposed based on monolithic cavity configuration [3–4].

In this letter, we propose a multi-section semiconductor laser with a monolithic cavity structure. The schematic representation of the proposed device is shown in Figure 1. The structure is considered to be a cascade of all-active three-section semiconductor lasers: two DFB lasers with uniform grating and with no-phase shifts at rear and front facets sections and a Fabry-Pérot laser in the middle. All the three sections have the same material and structural parameters (see Table 1) with an equal length and also biased with symmetrical driving current. We name this device as the monolithic three active-section (M3-As) laser.
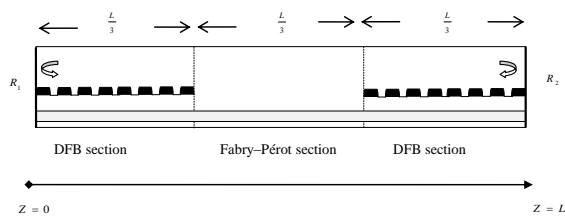

Fig. 1. Schematic representation of a M3-As semiconductor laser.

E-mail: bouchenemahdi@gmail.com

Table 1: Structural and material parameters.

Parameter	Value	Description	Unit
B_{spont}	1	Bimolecular coefficient	10^{-10} cm^3/s
C_{Aug}	3	Auger coefficient	10^{-29}cm^6/s
G_N	3	Differential field gain	10^{-16}cm^2
α_m	40	Waveguide loss	cm^{-1}
N_0	1.5	Transparency carrier density	10^{18}cm^3
n_{eff^0}	3.27	Effective phase refractive index	
n_g	3.7	Effective group refractive index	
L	400	Total cavity length	μm
w	3.5	Active layer width	μm
d	0.47	Active layer thickness	μm
Γ	0.35	Confinement factor	
R_2, R_1	0.32	Right and left facet power reflectivity	
λ_0	1550	Wavelength	nm
α_H	4.86	Linewidth enhancement factor	
ε	1	Gain compression factor	10^{-17}cm^3
β	10^{-4}	Spontaneous emission coefficient	

The theoretical framework used in our simulation is the one-dimensional Time Domain Travelling Wave (TDTW) model. The time-dependent coupled wave equations for the analysis different types of semiconductor lasers are expressed as follows [5]:

$$\frac{1}{C_G}\frac{\partial E^+}{\partial t} + \frac{\partial E^+}{\partial z} = \left(\frac{\Gamma G_N \{N - N_0\}}{2(1+\varepsilon S)} - \frac{\alpha_m}{2} - j\delta\right)E^+ + j\kappa E^- + \xi_+ \qquad (1)$$

$$\frac{1}{C_G}\frac{\partial E^-}{\partial t} - \frac{\partial E^-}{\partial z} = \left(\frac{\Gamma G_N \{N - N_0\}}{2(1+\varepsilon S)} - \frac{\alpha_m}{2} - j\delta\right)E^- + j\kappa E^+ + \xi_- \qquad (2)$$

In the above equations, $E^+(z,t), E^-(z,t)$ are respectively the forward and backward slowly varying amplitudes of

the traveling optical fields, and κ is the coupling coefficient between them. For a mixed-coupled DFB laser [6]: $\kappa = \kappa_i + j\kappa_g$, where κ_i is the index-coupling coefficient, and κ_g is the gain-coupling coefficient. For a purely index-coupled DFB laser, $\kappa_g = 0$, and for a purely gain-coupled DFB laser, $\kappa_i = 0$, and for a Fabry-Pérot laser, $\kappa = 0$. S is the photon density, α_m is the material loss, Γ is the confinement factor, δ is the detuning factor defined as:

$$\delta(z,t) = \frac{2\pi}{\lambda_0} n_{eff}(z,t) - \frac{\pi}{\Lambda} \ , \qquad (3)$$

n_{eff} is the effective refractive index, which is given by:

$$n_{eff}(z,t) = n_{eff}^0 - \Gamma \alpha_m \left(\frac{\Gamma G_N \{ N(z,t) - N_0 \}}{2(1 + \varepsilon S(z,t))}\right)\frac{\lambda_0}{4\pi} \ , \quad (4)$$

$\xi_+(z,t)$ and $\xi_-(z,t)$ are the spontaneous emission noises which are modeled in calculation by the Gaussian random number generator [7]. The rate equation for the carrier density N is given by [8]:

$$\frac{\partial N}{\partial t} = \frac{J(t)}{ed} - \frac{N}{\tau_s} - B_{Spont} N^2 - C_{Aug} N^3 - G C_G S \qquad (5)$$

where $J(t)$ is the injection current, e is the modulus of the electron charge, d is the volume of the active layer, τ_s is the carrier life time, B_{Spont} is the radiative spontaneous emission coefficient, C_{Aug} is the Auger recombination coefficient. The boundary conditions are defined at the rear and front facets of the laser as follows:

$$E^+((z=0),t) = \sqrt{R_1} E^-(z=0,t) \qquad (6)$$

$$E^-(z=L,t) = \sqrt{R_2} E^+(z=L,t) \qquad (7)$$

R_1, R_2 are the left and right facet power reflectivities. The TDTW model is solved explicitly in the time domain by using the Finite-Difference Time-Domain (FDTD) method [9]. The DFB lasers used in the M3-As configuration are gain-coupled grating because they show important advantages in terms of modal phase resonance as demonstrated in Fig. 2.
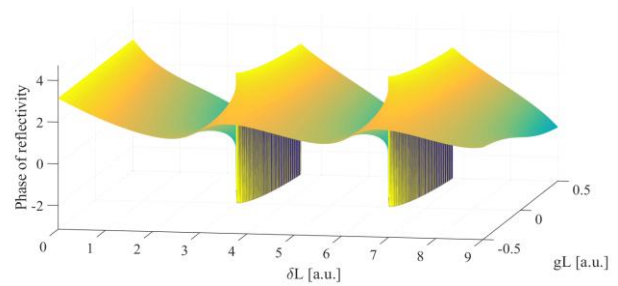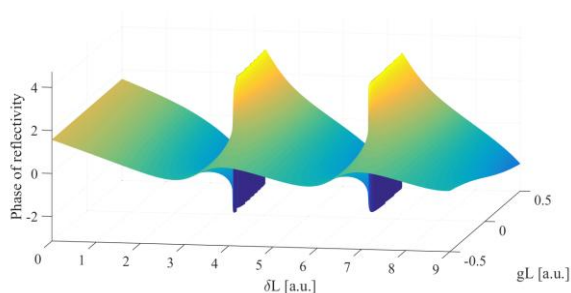

Fig. 2. Optical-field phase reflectivity in index and gain Bragg gratings.

Figure 3 shows the CW spectrum of an index-coupled DFB laser with $\kappa L = 2$ and a gain-coupled DFB laser and a M-3As laser biased at 51.15 mA. The emitted power from each facet for the three devices is respectively: 2.4830 mW, 4.3650 mW, and 5.0556 mW. The spectrum is obtained by applying the Fourier transform on the time samples of an optical field calculated by the TDTW model after the devices reach a steady-state condition [10]. It can be observed that the M3-As laser has the worst side-mode suppression ratio (SMSR). These results suggest that the M3-As laser is not suitable in a low output power range whereas the conventional DFB lasers show better performance.
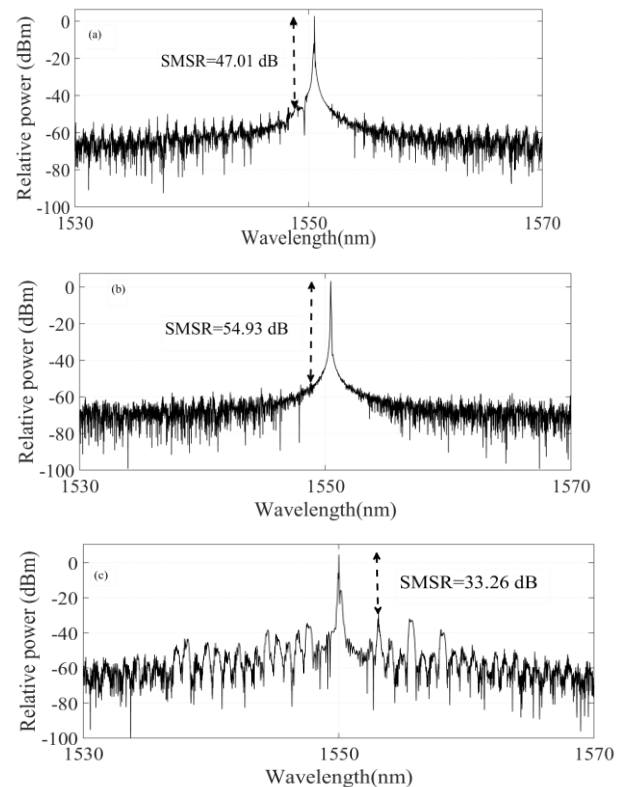

Fig. 3. CW optical spectra of: (a) an index-coupled DFB laser ($\kappa L = 2$), (b) a gain-coupled DFB laser, (c) a M3-As laser.

Figure 4 shows the CW spectra of an index-coupled ($\kappa L = 2$) laser, a gain-coupled DFB laser, and a M-3As laser biased at 250.78mA. The average power emitted from each facet for the three devices is respectively 25.4032mW, 34.9140mW, and 37.2348mW. It can be seen that both index- and gain-coupled DFB lasers have similar performance under strong injection current where the spectral linewidth has been drastically broaden and the laser exhibits a multimode operation as a result of strong longitudinal spatial-hole burning in a conventional DFB laser due to the modulation of the active layer refractive index caused by the change of carrier density which produces a dynamic frequency chirp in laser oscillation [11–12]. In contrary, the M3-As laser generates a single frequency oscillation and excellent wavelength stability at high output power with an improved side mode suppression ration equal to 56.08dB.
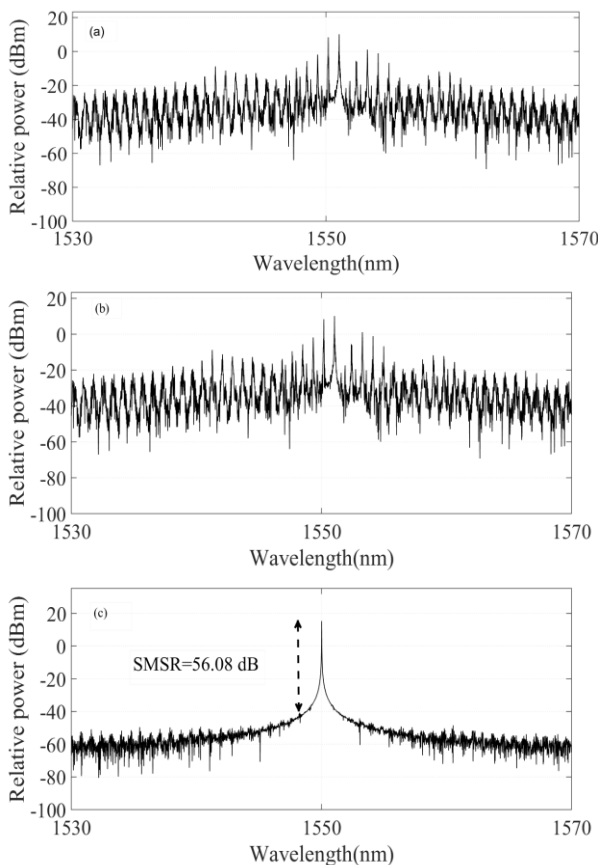

Fig. 4. CW optical spectra of: (a) an index-coupled DFB laser ($\kappa L = 2$), (b) a gain-coupled DFB laser, (c) a M3-As laser.

In order to confirm these results, we plot in Figure 5 the internal spatial distribution of optical intensity inside the laser (cavity) structure. As can be seen in the figure, the optical intensity in index- and gain-coupled DFB lasers builds up to achieve the maximum around the centre of the laser. Therefore, strong longitudinal spatial-hole burning occurs as the electron density decreases with the increase of the refractive index of the active region. On the other hand, it is clear that the M3-As laser has a near flat optical intensity profile; and this uniformity of optical field distribution is achieved by the uncorrugated section which represents the F-P laser section that creates a longitudinal field stop-band profile. This effect results in a significant reduction of longitudinal spatial-hole burning.
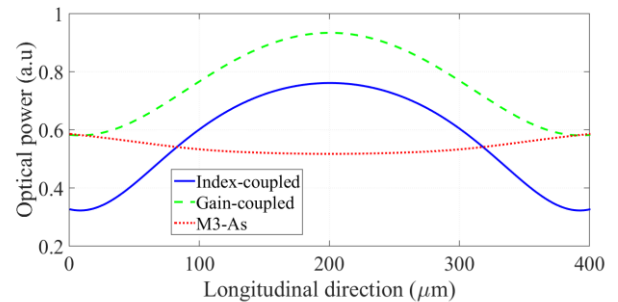

Fig. 5. Internal optical power distribution along the longitudinal direction of a M3-As laser.

In summary, we have investigated theoretically the novel structure of a monolithic multi-section semiconductor laser operating around a wavelength of 1550nm. Single-frequency operation for a relatively high output power emission has been successfully achieved. The results suggest that the M3-As laser could be used in applications that require a high output power narrow-linewidth.

References

[1]   L.A. Coldren, IEEE J. Select. Topics Quant. Electron. **6**, 988 (2000).
[2]   O. Kjebon, R. Schatz, S. Lourdudoss, S. Nilsson, B. Stalnacke, L. Backbom, Electron. Lett. **33**(6), 488 (1997).
[3]   N. Kim, J. Shin, E. Sim, C.W. Lee, D.-S. Yee, M.Y. Jeon, Y. Jang, K.H. Park, Opt. Expr. **17**(16), 13851 (2009).
[4]   M.J. Wallace, R. ORreilly Meehan, R.R Enright, F. Bello, D. Mccloskey, B. Barabadi, E.N. Wang, J.F. Donegan, Opt. Expr. **25**(13), 14426 (2017).
[5]   J.E. Carroll, J.E.A. Whiteaway, R.G.S. Plumb, *Distributed feedback semiconductor lasers* (IEE and SPIE, 1998).
[6]   H. Ghafour-Shiraz, *Distributed Feedback Laser Diodes and Optical Tunable Filters* (Wiley, 2003).
[7]   D.D. Marcenac, Ph.D dissertation (University of Cambridge, 1993).
[8]   L.M. Zhang, J.E. Carroll, C. Tsang, IEEE J. Quant. Electr. **29**, 1722 (1993).
[9]   W. Li, W.-P. Huang, X. Li, J. Hong, IEEE J. Quant. Electro. **36**(10), 1110 (2000).
[10] B.M. Mehdi, H. Rachid, in Proc. 3rd Intern. Conf. on Embedded Systems in Telecomm. and Instrument., Annaba, Algeria (2016).
[11] C. Henry, IEEE J.Quant. Electr. **QE-18**, 259 (1982).
[12] K. Takaki, T. Kise, K. Maruyama, N. Yamanaka, M. Funabashi, A. Kasukawa, IEEE J. Quant. Electr. **39**, 1060 (2003).